Functionally Important Interactions between the Nucleotide-Binding Domains of an Antigenic Peptide Transporter[†]

Erik Procko and Rachelle Gaudet*

Department of Molecular and Cellular Biology, Harvard University, 7 Divinity Avenue, Cambridge, Massachusetts 02138

Received December 20, 2007; Revised Manuscript Received March 1, 2008

ABSTRACT: The transporter associated with antigen processing (TAP), an ABC transporter, pumps cytosolic peptides into the endoplasmic reticulum, where the peptides are loaded onto class I MHC molecules for presentation to the immune system. Transport is fueled by the binding of ATP to two cytosolic nucleotide-binding domains (NBDs) and ATP hydrolysis. We demonstrate biochemically that there are two electrostatic interactions across the interface between the two TAP NBDs and that these interactions are important for peptide transport. Notably, disrupting these interactions by mutagenesis does not greatly alter the ATP hydrolysis rate in an isolated NBD model system, suggesting that the interactions function at alternative stages in the transport cycle. The data support the general model for ABC transporters in which the NBDs form a tight, closed conformation during transport. Our results are discussed in relation to other ABC transporters that do or do not conserve potential interacting residues of opposite charges at the homologous positions.

ATP-binding cassette (ABC)[1] family transporters use ATP to shuttle substrate across a membrane. ABC transporters have a large diversity of substrates, including small charged ions, hydrophobic toxins, or even polypeptide chains, yet all share a similar modular architecture and likely a similar mechanism. Four domains form a "core" transporter, although many eukaryotic transporters have additional accessory domains for regulation or protein−protein interactions (*1*−*3*). The core domains include two transmembrane domains (TMDs) which form the translocation pathway across the membrane and two cytosolic nucleotide-binding domains (NBDs) which couple ATP binding and hydrolysis to the necessary conformational changes for transport. Specifically, ATP binding to each NBD causes the NBDs to interact, with the two ATP molecules sandwiched at the interface and bridging contacts between the two NBDs (*4, 5*). Following ATP hydrolysis, the NBD dimer reopens, allowing the cycle to repeat. This opening and closing of the NBD dimer facilitates conformational changes in the associated TMDs, including switching from an inward- to outward-facing state and generation of a translocation pathway (*6*−*8*).

The transporter associated with antigen processing (TAP) is an ABC transporter that exports cytosolic peptides derived from ubiquitin/proteasome-mediated degradation into the endoplasmic reticulum (ER) (*9, 10*). These peptides are bound by class I MHC molecules which then exit the ER and decorate the cell surface, where they are scanned by the immune system for evidence of virus infection, cancer, or other maladies (*11*). TAP is a heterodimer of TAP1 and TAP2 subunits (*12*), which each contribute a TMD and an NBD to form the core transporter unit, as well as an additional N-terminal accessory domain that assembles a higher-order peptide-loading complex with class I MHC and tapasin (a class I-specific chaperone) (*2, 13*).

Following ATP binding, the TAP1- and TAP2-NBDs are hypothesized to form the aforementioned ATP sandwich dimer, with each ATPase active site composed of residues from both TAP1 and TAP2. Frequently in heterodimeric transporters, including TAP, one ATPase site is comprised of conserved, consensus residues for ATP binding and hydrolysis, while the second site contains nonconsensus substitutions in these important motifs (*14*). These are termed the consensus and degenerate ATPase sites, respectively. Using a TAP1-NBD homodimer as a scaffold to construct various ATPase sites, we previously showed that the consensus site is the principal driver of ATP hydrolysis and NBD closure/dimerization (*14*). An appealing hypothesis is that ATP hydrolysis is ordered and sequential, with the more active consensus site firing first, followed by the degenerate site (*14, 15*). Other residues nearby or outside the two ATPase sites may coordinate to allow cross-talk and tighter regulation between the two sites.

One study that partially addressed this idea of cross-talk between the ATPase sites investigated the bacterial ABC transporter HlyB (*16*). The crystal structure of the ATP-bound NBD dimer of HlyB exhibits pseudo-2-fold symmetry, with differences within a cavity near the γ-phosphate of each ATP (*16*). At one ATPase site, $Asp551_A$ and $Arg611_A$ are 3.3 Å apart and constrict this cavity, while at the second site, $Asp551_B$ and $Arg611_B$ are farther apart (4.7 Å) and the cavity is widened ("A" and "B" subscripts refer to the two

[†] This project was supported by the American Cancer Society (Grant RSG GMC-111847 to R.G.). E.P. is supported by a Merck-Wiley Fellowship.

* To whom correspondence should be addressed. Fax: (617) 496-9684. Phone: (617) 495-5616. E-mail: gaudet@mcb.harvard.edu.

[1] Abbreviations: ABC, ATP-binding cassette; ER, endoplasmic reticulum; HLA, human leukocyte antigen; MHC, major histocompatibility complex; NBD, nucleotide-binding domain; PDB, Protein Data Bank; SD, standard deviation; TAP, transporter associated with antigen processing; TMD, transmembrane domain; V_e, elution volume.

10.1021/bi7024854 CCC: $40.75
Published on Web 05/02/2008

NBD subunits) (*16*). Since this cavity is near the γ-phosphate, this was interpreted as asymmetric opening and closing of a phosphate exit tunnel such that hydrolysis can only proceed at a single site until a subsequent conformational change facilitates hydrolysis at the second site. It was suggested that the site with an open tunnel would hydrolyze first (*16*), although an alternative hypothesis is that the site near the closed cavity may better surround and stabilize the reaction transition state and facilitate catalysis. Mutation of either Asp551 or Arg611 to alanine eliminated ATP-dependent cooperativity in ATPase assays, implicating these residues in cross-talk between the two ATPase sites (*16*). We hence decided to investigate the equivalent residues in TAP.

In this report, we demonstrate that these conserved residues form two functionally important interactions across the TAP1-NBD/TAP2-NBD dimer interface. These data support the existence of the closed, dimeric state of the TAP-NBDs presumed to exist during the transport cycle. We further demonstrate that the basic residues of the interacting pairs have additional roles in promoting NBD closure. However, disruption of the interactions in the isolated TAP1-NBD dimer does not cause severe defects in ATPase activity, suggesting the interactions function at stages other than ATP hydrolysis during transport. The idea of cross-talk and implications of our data for other ABC transporters are discussed.

EXPERIMENTAL PROCEDURES

Plasmid Construction and Protein Purification. The cloning of the rat TAP1-NBD (residues 466−725) into pET21(a) (Novagen) with a C-terminal six-His tag and full-length rat TAP into pFastBacDual (Invitrogen) with C-terminal six-His and FLAG tags on TAP1 and TAP2, respectively, has previously been described (*14*). Site-specific substitutions were introduced by sequence overlapping PCR, and all plasmid sequences were confirmed by DNA sequencing (MWG Biotech). TAP1-NBD proteins were expressed, purified, and stored as previously described (*14*).

Tissue Culture and Class I MHC Loading Assay. Sf21 insect cells were cultured at 27 °C in Hink's TNM-FH with 10% fetal bovine serum and 0.1% pluronic F-68 (Mediatech). Bacmid DNA and baculoviruses were prepared according to the Bac-to-Bac system manual (Invitrogen). Protein expression levels were determined by SDS−PAGE, immunoblotting with anti-His (C-term)/AP (Invitrogen) or anti-FLAG M2 antibody/AP (Sigma), and developing with NBT/BCIP (Pierce). Reconstitution of the class I MHC loading pathway and detection of surface class I MHC by flow cytometry are previously described (*2*).

Nucleotide Binding Assay. Ten micrograms of TAP1-NBD was diluted to 1 mL in binding buffer [130 mM NaCl, 10 mM Na_2HPO_4, 5 mM $MgCl_2$, 0.3% decyl β-D-maltopyranoside, 1 mM DTT, and 10 mM Tris (pH 7.5)] and incubated with 3.75 mg of nucleotide-conjugated agarose [pre-equilibrated in 100 mM Tris (pH 7.5) and 500 mM NaCl; nine-atom linker to C-8; Sigma] for 1 h at 4 °C. The nucleotide-agarose beads were washed three times with 0.9 mL of binding buffer and resuspended in 200 μL of SDS sample loading dye. Samples were analyzed by electrophoresis on 12% SDS gels and stained with Coomassie Brilliant Blue.

Size Exclusion Chromatography. Dimerization of TAP1-NBDs (6.5 mg) was investigated by size exclusion chromatography on a Superdex200 16/60 column (GE Healthcare) at 1 mL/min. The running buffer [50 mM NaCl, 5 mM $MgCl_2$, 10% glycerol, 1 mM DTT, and 20 mM Tris (pH 8.0)] was supplemented with 1 mM ADP (Sigma) or 1 mM ATP (Sigma) as indicated.

ATPase Reaction Assay. TAP1-NBD protein samples were exchanged two or three times into ATPase reaction buffer [150 mM potassium acetate, 10% glycerol, 1 mM DTT, and 50 mM K-HEPES (pH 7.5)] by size exclusion chromatography with a Superdex200 16/60 column, until the Ab_{260}/Ab_{280} ratio was ~0.6. The proteins (16 μM) were prepared in ATPase reaction buffer containing 8 mM magnesium acetate, 0.25 mg/mL BSA, 0.1 unit/mL lactate dehydrogenase (Sigma), 6 units/mL pyruvate kinase (Sigma), 4 mM phosphoenolpyruvate (Sigma), and 0.32 mM NADH (Sigma) and aliquoted in 200 μL volumes into UV-transparent 96-well trays. Different ATP concentrations were established by serial dilution. NADH oxidation was measured by the decrease in absorbance at 340 nm on a SpectraMax M5 spectrophotometer (Molecular Devices), for 90 min at 25 °C, with readings every 30 s. The rate of hydrolysis was determined as $[-\Delta(Ab_{340})/\Delta t]/6.22$ mM min^{-1}, where 6.22 $mM^{-1}cm^{-1}$ is the NADH extinction coefficient, and data were fitted to the Hill equation using IGOR Pro 6 (WaveMetrics).

RESULTS

Mutagenesis of Interacting Residues in the TAP1-NBD Dimer. While a structure of an ATP-bound TAP1-NBD/TAP2-NBD heterodimer has yet to be determined, we previously described a structure of a nonphysiological TAP1-NBD homodimer with ATP (*14*). Experiments using the TAP1-NBD dimer as a model system successfully predicted and explained results in the full-length TAP transporter (*14*). Analysis of the 2.0 Å dimeric TAP1-NBD structure (PDB entry 2IXE) reveals asymmetry near each ATP (Figure 1A,B). $Glu564_A$ makes a water-mediated hydrogen bond to $Arg625_B$, equivalent to the "closed tunnel" described for HlyB (*16*), while at the second ATPase site, $Glu564_B$ is disordered and multiple conformations were modeled for $Arg625_A$, an extreme example of an "open tunnel". Glu564 and Arg625 of TAP1 are homologous to Asp551 and Arg611 of HlyB, respectively. Of note, in the ATP-bound conformation of the full-length bacterial ABC transporter Sav1866 (*17, 18*), the homologous residues (Asp423 and Lys483) interact across the dimer interface like Glu564 and Arg625 in the TAP1-NBD dimer (Figure 1C). However, in Sav1866, the TMDs push NBD loops on the contact surface inward such that Asp423 and Lys483 interact directly in a salt bridge. In the TAP1-NBD dimer, surface loops that would contact the TAP TMDs are poorly ordered, and in the full transporter, the acidic and basic residues may interact directly in a salt bridge similar to that observed in Sav1866. In both TAP1-NBD and HlyB-NBD structures, these interacting residues close off one ATPase site, while the second ATPase site is more accessible with the charged residues farther apart or disordered. [In the lower-resolution Sav1866 structure, strict noncrystallographic symmetry constraints were imposed during refinement (*17, 18*), precluding any conclusions about asymmetry at the NBD interface.] However, an important

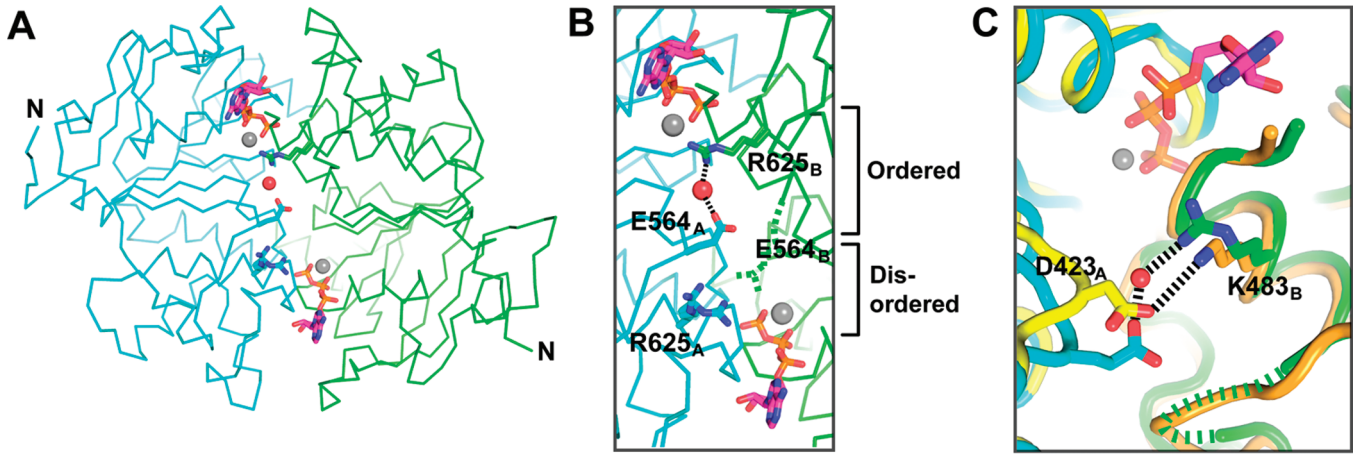

D

Protein	Species	Q-loop	Signature
TAP1	Human	584 VGQEP	643 LSGGQR
	Rat	561 VGQEP	620 LSGGQR
	Shark	558 VSQEP	617 LSGGQK
	Xenopus	553 VSQEP	611 LSVGQK
TAP2	Human	549 VGQEP	606 LAAGQK
	Rat	549 VGQEP	607 LAVGQK
	Shark	551 VGQEP	609 LSAQQK
	Chicken	547 VGQEP	605 LSAGQK
BSEP	Human	501 VEQEP	559 MSGGQK
		1159 VSQEP	1219 LSRGEK
MRP4	Human	478 VSQQP	535 LSGGQK
		1120 IPQEP	1177 FSVGQR
SUR1	Human	771 ASQKP	828 LSGGQR
		1423 ILQDP	1480 FSQGQR
MalK	E. coli	80 VFQSY	134 LSGGQR
Sav1866	S. aureus	420 VQQDN	478 LSGGQK
HlyB	E. coli	548 VLQDN	606 LSGGQR

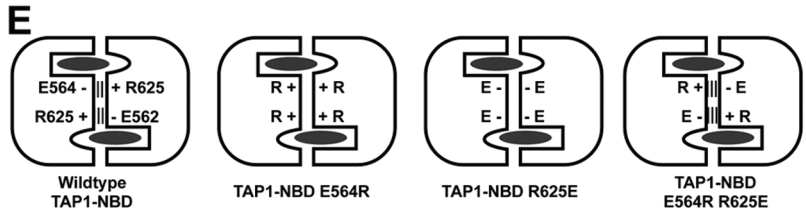

FIGURE 1: Asymmetric arrangement of interactions across the ATP-bound dimeric TAP1-NBD interface. (A) Structure of the ATP-bound TAP1-NBD dimer [PDB entry 2IXE (*14*)]. The Cα traces of the two subunits are colored cyan (subunit A) and green (subunit B), and ATP/Mg^{2+} is colored magenta. (B) The interface is magnified to show that the Glu564−Arg625 interaction occurs intermolecularly across the interface via a water molecule (red sphere) and is ordered near one ATP molecule and disordered near the second. (C) The structure of the ATP-bound TAP1-NBD dimer (same color scheme as in panel A) is superimposed with Sav1866 [light and dark yellow; PDB entry 2ONJ (*18*)]. In Sav1866, Asp423 forms a salt bridge across the interface with K483. The Q-loops of the TAP1-NBD dimer are shifted (subunit A, cyan) or disordered (subunit B, green dotted line) compared to Sav1866, where these loops are held in place by contacts with the TMDs. (D) Table of the Q-loop and signature motif sequences of TAP proteins from various species and other ABC transporters. The conserved acidic residue of the Q-loop and the basic residue adjacent to the signature motif are highlighted in red. The residues of rat TAP1 and TAP2 mutated in this study are boxed. (E) Schematic representations of the different TAP1-NBD mutants constructed. The dark gray ovals represent ATP.

difference is that while salt bridges occur intramolecularly within each HlyB subunit, in TAP1-NBD (and also in Sav1866) the interactions cross the dimer interface in an intermolecular fashion. Since the four charged residues are in the proximity of one another (Figure 1B and Supporting Information, Figure S1), both of these two distinct arrangements are possible.

The charged residues in the TAP1-NBD homodimer correspond to Glu564 and Arg625 of TAP1 and Glu552 and Lys612 of TAP2 and are conserved across species, as expected if they have an important function (Figure 1D). We considered three possibilities in extrapolating these electrostatic interactions to a putative TAP1-NBD/TAP2-NBD heterodimer: (i) functional intersubunit salt bridges as observed in the TAP1-NBD and Sav1866 dimers, (ii) functional intrasubunit interactions as observed in the HlyB-NBD dimer, and (iii) all four charged residues forming an extended salt bridge network, with different electrostatic interactions forming along or across the dimer interface during the transport cycle. In all three scenarios, an interac-

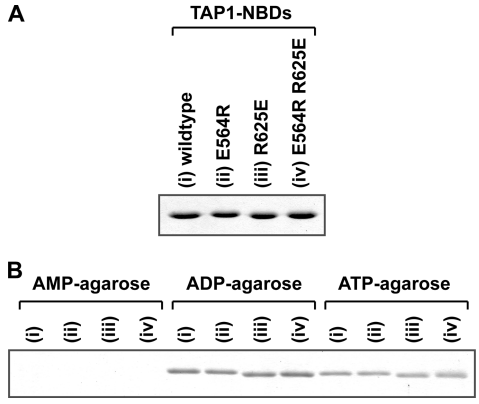

FIGURE 2: TAP1-NBD interaction mutants bind nucleotide-agarose similarly. Nucleotide binding was qualitatively assessed by precipitating purified TAP1-NBD proteins with nucleotide-coupled agarose. (A) Coomassie-stained SDS−polyacrylamide gel of the protein loads. (B) Protein bound to the nucleotide-agarose beads was eluted by boiling in SDS sample buffer and analyzed on a Coomassie-stained SDS gel. Shown are representative results from three separate experiments.

tion that closes off one ATPase site might require the adjacent interaction to be open at the second site, as observed in both the TAP1-NBD and HlyB-NBD structures. This would provide a mechanism for cross-talk between the two ATPase sites.

To examine the role of these charged residues in a tractable model system, mutations were introduced into TAP1-NBD, replacing Glu564 or Arg625 with an oppositely charged arginine (E564R) or glutamate (R625E), respectively (Figure 1E). The double mutation in TAP1-NBD, E564R/R625E, restored the interacting components in the opposite orientation (Figure 1E). The premise was to look for loss of function with the single mutants and then a rescue of function when the interaction was restored in the opposite orientation.

In a qualitative test of nucleotide binding affinity, the TAP1-NBD constructs were precipitated by nucleotide-coupled agarose (Figure 2A,B). The wild-type (WT) TAP1-NBD and all three mutants were similarly precipitated by ADP- and ATP-agarose, but not AMP-agarose. That the proteins display similar nucleotide binding specificities and retain ATPase activity (described later) rules out the possibility that the mutations cause gross structural changes.

ATPase Activity of the TAP1-NBD Mutants. When the equivalent interactions were disrupted in HlyB-NBD, ATPase activity was reduced and ATP-dependent positive cooperativity was lost (*16*). To determine if loss of the TAP1-NBD interfacial interactions has a similar effect, ATPase activity of the TAP1-NBD constructs was measured by a coupled reaction assay (Figure 3). Due to the instability of TAP-NBDs in the absence of nucleotide, constructs were purified and stored in the presence of 1 mM ATP, which was removed by multiple size exclusion chromatography runs immediately before the assay. The maximum velocity of the ATPase reaction (V_{max}) varied from 0.85 ± 0.01 to 1.90 ± 0.07 μM ATP/min, and Hill coefficients for ATP-dependent cooperativity varied from 1.28 ± 0.05 to 1.55 ± 0.03 (Figure 3). If the interactions influenced enzymatic parameters, it was expected that the E564R and R625E mutants would exhibit similar altered behavior, while the double E564R/R625E mutant would restore wild-type properties. Differences in V_{max} and Hill coefficients did not follow a trend consistent with a role for the Glu564−Arg625 interaction. However, the $K_{1/2}$ constant (the ATP concentration at which the velocity is half of V_{max}) was reduced in TAP1-NBD E564R ($K_{1/2}$ = 13.8 ± 0.03 μM) and R625E ($K_{1/2}$ = 13.5 ± 0.02 μM) mutants compared to the wild type (WT) ($K_{1/2}$ = 20 ± 2 μM) and E564R/R625E ($K_{1/2}$ = 23 ± 3 μM) proteins, suggesting that interfacial Glu564−Arg625 interactions increase the $K_{1/2}$ value, i.e., lower the apparent affinity for ATP. However, considering that the intracellular ATP concentration [2−7 mM (*19*)] is much higher than the $K_{1/2}$ constants, it is unclear if this has any significance for TAP under physiological conditions. Overall, these ATPase activity measurements reveal no major role for the interactions.

Dimerization of the TAP1-NBD Mutants. In the presence of 1 mM ATP, TAP1-NBD forms a transient dimer eluting at a higher apparent molecular weight (MW) from a size exclusion chromatography column [peak elution volume (V_e) of 82.0 mL] compared to monomeric ADP-bound TAP1-NBD (V_e = 86.3 mL) (Figure 4A). The shift to a higher apparent MW depends on both TAP1-NBD dimer stability and the ATP hydrolysis rate (*14*). Since the TAP1-NBD mutants analyzed here have similar ATPase activity, size exclusion chromatography analysis likely reflects differences in dimer stability. The TAP1-NBD E564R mutant eluted at a higher apparent MW (V_e = 81.3 mL) than WT with ATP (Figure 4B), suggesting that the dimer stability is increased. However, the ATP-bound TAP1-NBD R625E dimer is less stable than WT [V_e = 83.6 mL (Figure 4C)]. Both mutants disrupt the Glu564−Arg625 interactions, yet they cause opposite effects. Instead, dimer stability correlates with the ratio of basic to acidic residues; the additional positive charge at the interface of the E564R mutant may stabilize a dimer held together by negatively charged ATP. The double mutant, TAP1-NBD E564R/R625E, restores the wild-type ratio of basic to acidic interfacial residues and has an elution profile in the presence of ATP similar to that of WT [V_e = 82.4 mL (Figure 4D)].

Mutagenesis of Interfacial Interactions in the Full-Length TAP Transporter. While the interfacial interactions did not significantly influence the ATPase activity of the isolated TAP1-NBD, the interactions may have other important roles, such as transmitting conformational signals between the NBDs and TMDs or orchestrating the correct series of events during the transport cycle. Moreover, these interactions, hypothesized on the basis of the TAP1-NBD structure, may have a different arrangement in the full transporter. To address these possibilities, full-length TAP transport activity was measured in Sf21 insect cells by reconstituting the class I MHC loading pathway heterologously. The detection of surface class I molecules with a fluorescent antibody by flow cytometry is an indirect indicator of TAP transport activity, as only peptide-loaded class I molecules can escape the ER (*20*). Loading of peptide onto two different human class I alleles was examined: human leukocyte antigen (HLA)-B*4402 and HLA-B*2705. HLA-B*4402 requires the specialized class I-specific chaperone tapasin for proper folding and surface expression, whereas HLA-B*2705 does not (*2, 21*).

On the basis of the TAP1-NBD dimer, two electrostatic interactions were predicted across the heterodimeric TAP interface: Glu564[TAP1]−Lys612[TAP2] and Arg625-[TAP1]−Glu552[TAP2]. To determine if these interactions

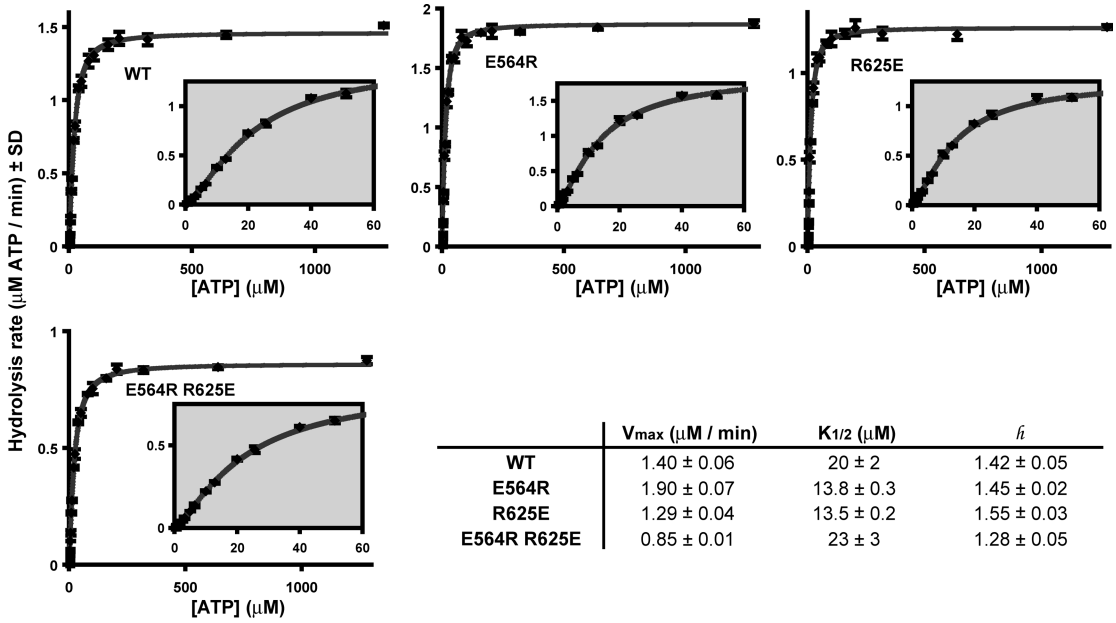

	V_{max} (μM / min)	$K_{1/2}$ (μM)	*h*
WT	1.40 ± 0.06	20 ± 2	1.42 ± 0.05
E564R	1.90 ± 0.07	13.8 ± 0.3	1.45 ± 0.02
R625E	1.29 ± 0.04	13.5 ± 0.2	1.55 ± 0.03
E564R R625E	0.85 ± 0.01	23 ± 3	1.28 ± 0.05

FIGURE 3: ATPase activity of the TAP1-NBD proteins at 16 μM measured by a coupled reaction assay at 25 °C. The graphs show representative results from three separate experiments each in triplicate. The average values for the kinetic parameters from all experiments, calculated from the trend lines that satisfy the Hill equation $v = (V_{max}[ATP]^h)/([ATP]^h + K_{1/2}{}^h)$, are shown in the table. V_{max} is the maximum velocity, [ATP] the ATP concentration, $K_{1/2}$ the ATP concentration at which the velocity is half of V_{max}, and *h* the Hill coefficient (cooperativity with respect to ATP concentration).

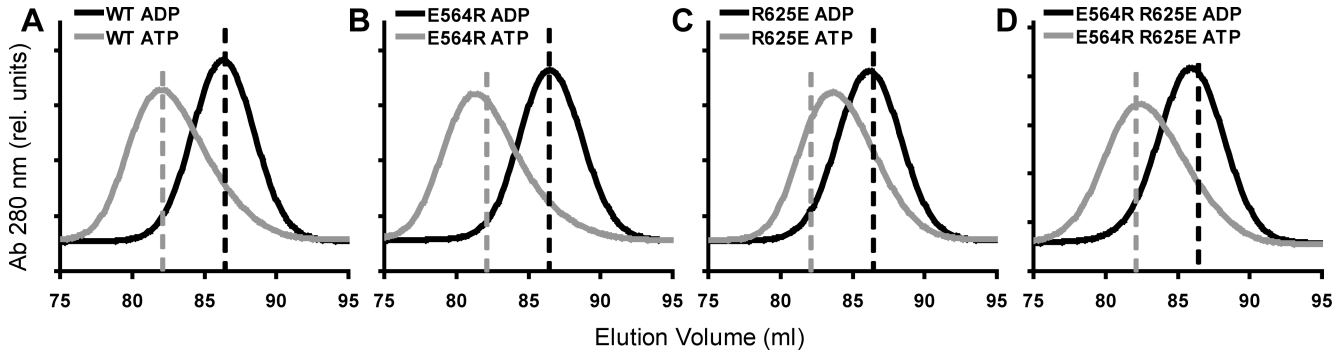

FIGURE 4: Purified TAP1-NBD proteins were analyzed on a Superdex200 16/60 size exclusion chromatography column in the presence of 1 mM ADP (black) or ATP (gray). The vertical dashed lines indicate the peak elution volumes of wild-type TAP1-NBD with ADP (black, 86.3 mL) or ATP (gray, 82.0 mL) for reference. Shown are representative traces from two to four experiments for wild-type (A), E564R (B), R625E (C), and E564R/R625E (D).

occur and are functional, each residue was mutated in full-length TAP to an amino acid of the opposite charge, and then a second mutation was introduced to restore the interaction in the opposite orientation. The various mutants are diagrammed in Figure 5A, and their class I MHC loading activity is shown in panels B (HLA-B*2705 allele) and C (HLA-B*4402 allele) of Figure 5. There are four important conclusions from the data. First, mutagenesis of any of these residues impairs TAP transport activity. Second, the transport activity defect is much worse when the basic residue is mutated (i.e., TAP1 R625E or TAP2 K612E). Third, the double mutants with restored intersubunit interactions in the opposite orientation both show partial rescue. In the case of TAP1 E564K/TAP2 K612E, transport is rescued to levels above each of the single mutants alone. For TAP1 R625E/TAP2 E552R, activity is rescued to levels above the weakest of the single mutants (TAP1 R625E/TAP2). This rescue of activity strongly supports the presence of ionic interactions between Glu564[TAP1] and Lys612[TAP2] and between Arg625[TAP1] and Glu552[TAP2] and indicates that TAP1-NBD and TAP2-NBD form a dimer similar to the ATP-bound TAP1-NBD dimer at some point during the transport cycle. Fourth, the results are similar whether mutations are introduced at the consensus ATPase site or the degenerate site. This is distinct from mutations that destroy ATP binding and/or hydrolysis, which are much worse when introduced at the consensus site (*15, 22, 23*). Therefore, even though the two ATPase sites have quite different properties, they are still both important for peptide transport.

The previous data demonstrate that specific acidic and basic residues form functional interactions across the TAP interface. To determine if there are also functional intrasubunit interactions as observed in the ATP-bound HlyB-NBD dimer (i.e., Glu564−Arg625 of TAP1 and Glu552−Lys612 of TAP2), we used the same mutagenesis approach and looked for complementation by double mutations that restore a potential intrasubunit interaction in the opposite orientation (Figure 6A). As before, single mutations all reduced transport activity (Figure 6B,C). However, the double mutants (TAP1 E564K R625E/TAP2 and TAP1/TAP2 E552R K612E)

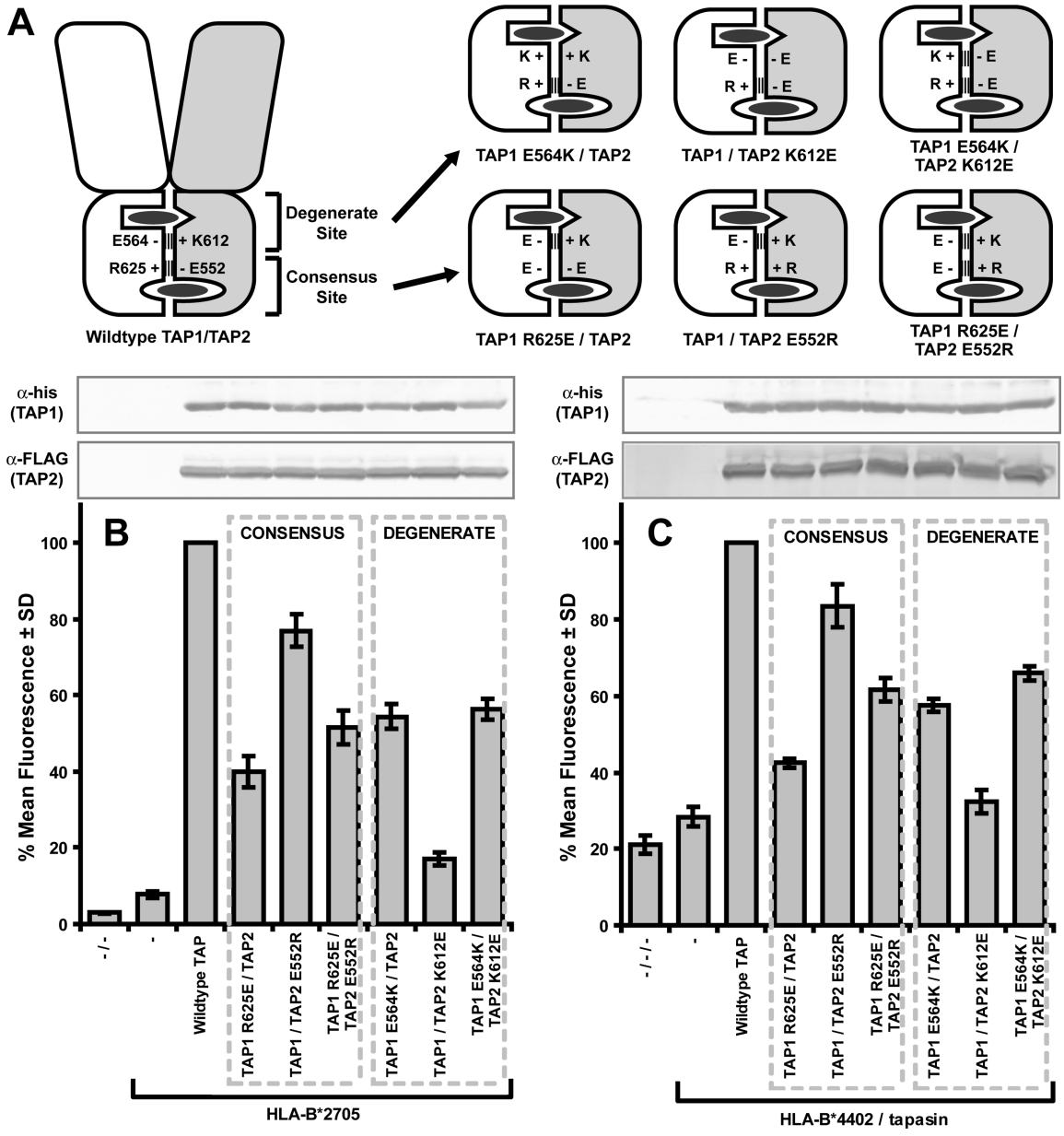

FIGURE 5: Charged residues interact intermolecularly across the TAP interface. (A) Schematic representations of mutations introduced into full-length rat TAP. On the left is wild-type TAP, while on the right are shown the mutations on the NBDs only. Dashed lines across the interface indicate putative interactions, and dark gray ovals represent ATP. (B) The class I MHC loading pathway was reconstituted in Sf21 insect cells by co-infecting them with two baculoviruses encoding HLA-B*2705 and β_2-microglobulin, and TAP1 and TAP2, respectively. Surface class I expression was assessed by flow cytometry. Shown is the average from four separate experiments ± SD. Fluorescence values are expressed as a percentage of the fluorescence from cells expressing wild-type TAP. Mutations that disrupt predicted intersubunit salt bridges near the consensus and degenerate ATPase sites are indicated. Western blots show that expression of the different TAP mutants was similar (lanes are vertically aligned with the bar graph). (C) As in panel B, except that triple-infected Sf21 cells were expressing HLA-B*4402 and tapasin instead of HLA-B*2705. Shown is the average from five separate experiments ± SD.

suffered a further decline in activity and were essentially inactive. When two additional mutations were introduced to restore the intersubunit interactions across the interface (TAP1 E564K R625E/TAP2 E552R K612E; all four charged residues have been exchanged), then transport was slightly rescued. This was most evident for samples expressing the HLA-B*4402 allele with tapasin, where fluorescence increased from 40 ± 3 and 41 ± 2% for the two double mutants up to 50 ± 2% of the maximum fluorescence when all four residues were mutated. Again, the data support intersubunit interactions across the TAP1-NBD/TAP2-NBD interface, while there is no evidence of intrasubunit interactions. In addition, since rescue of transport activity was only partial, there is also a preferred orientation of the interacting residues (i.e., for residues of a specific charge to be in a specific position).

DISCUSSION

By determining whether two mutated residues can complement each other and at least partially rescue activity, we have shown that TAP has two intersubunit interactions between Glu564 of TAP1 and Lys612 of TAP2 and between Arg625 of TAP1 and Glu552 of TAP2 (Figure 7A). Such interactions were predicted from the dimeric ATP-bound TAP1-NBD and AMP-PNP-bound Sav1866 crystal structures (*14, 18*), and

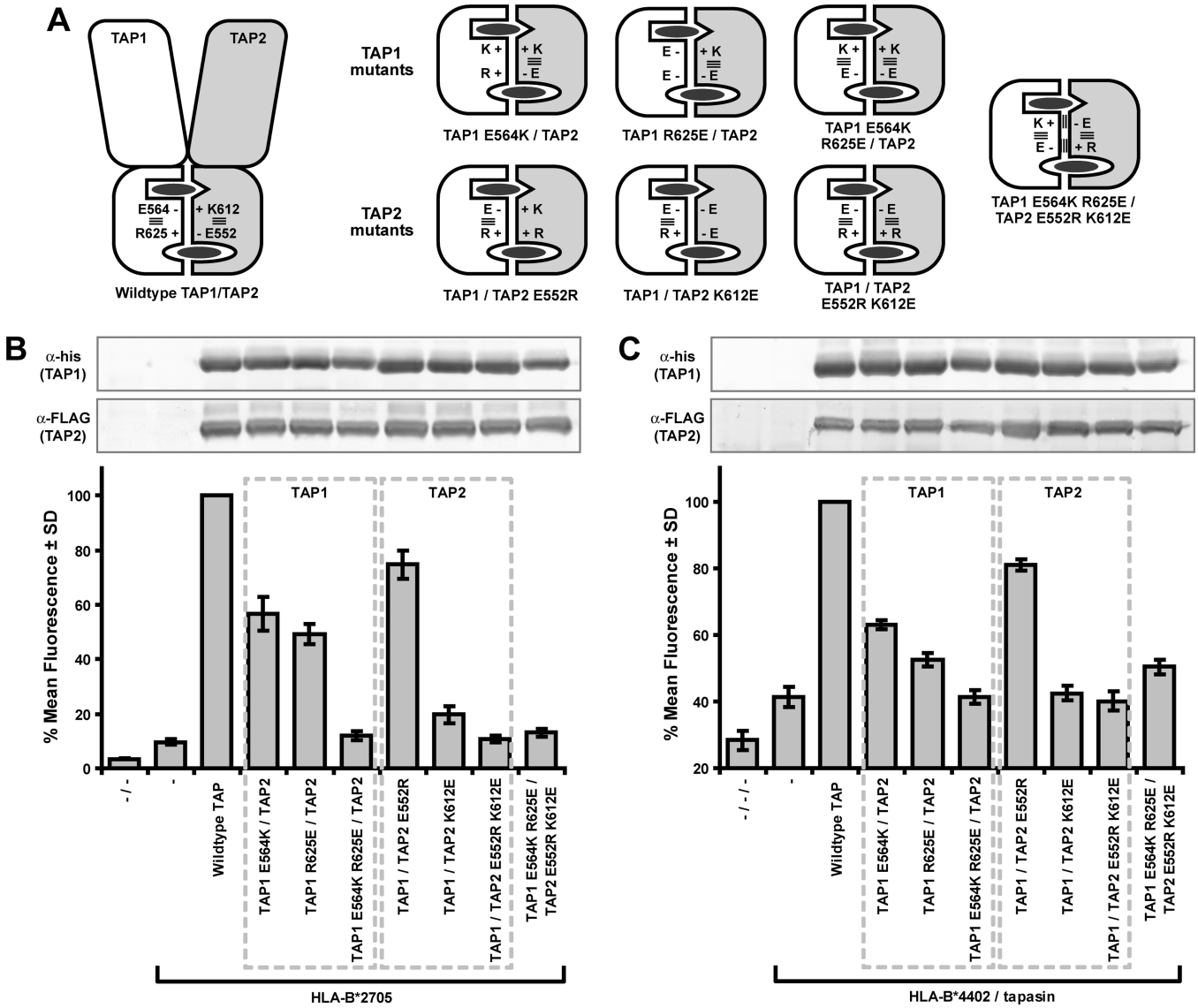

FIGURE 6: No evidence for intramolecular interactions. (A) Schematic representations of mutations introduced into full-length rat TAP similar to those in Figure 5A. (B) The class I MHC loading pathway was reconstituted in Sf21 insect cells expressing mutants of TAP and HLA-B*2705. Single mutations exchanging acidic and basic residues were compared to double mutants where two residues, both on the same subunit as indicated by the dashed boxes, were exchanged. The average fluorescence ± SD from three separate experiments is shown as a percentage of the signal from cells expressing wild-type TAP. Western blots are shown above, and lanes are vertically aligned with the bar graph. (C) Like panel B, except cells were infected with baculoviruses encoding HLA-B*4402 and tapasin instead of HLA-B*2705.

our results strongly support the model in which the TAP1- and TAP2-NBDs form a similar dimer at some point during a transport cycle. While these charged residues and their interactions are important for substrate transport, studies of the TAP1-NBD dimer revealed no major roles for the interactions during ATP hydrolysis or NBD dimerization, suggesting that the putative salt bridges have important function(s) at other stages during transport. Further, since the trends in peptide loading assays were essentially the same with tapasin-dependent and tapasin-independent class I MHC alleles for all mutants, the interactions probably do not have a major role in communicating with tapasin, yet mutating the interacting residues had a dramatic deleterious effect on TAP transport activity. The effect is even more severe than that observed for many mutations that reduce ATPase activity or mutations to the signature motif that weaken NBD dimerization to a far greater extent than the slight changes to dimer stability observed here (*14* and references therein), clearly suggesting an important function.

One hypothesis is that the electrostatic interactions have a role in transmitting motions from the NBDs to the TMDs or vice versa. The acidic residues we investigated are immediately adjacent to the conserved glutamine of the Q-loop (Figure 1D), which changes position markedly as the two NBD subdomains shift and the NBDs separate following ATP hydrolysis (*24, 25*). In Sav1866, the Q-loop contacts the intracellular surface of the TMD and is thought to communicate NBD motions to the TMDs (*17*). In our structural model, each Q-loop is tethered by one of these interactions, which must break for the NBDs to separate.

A second possibility arises from the observation that the interacting pairs of both the degenerate and consensus ATPase sites are important for transport. This is in contrast to mutations that block ATP binding or hydrolysis, which

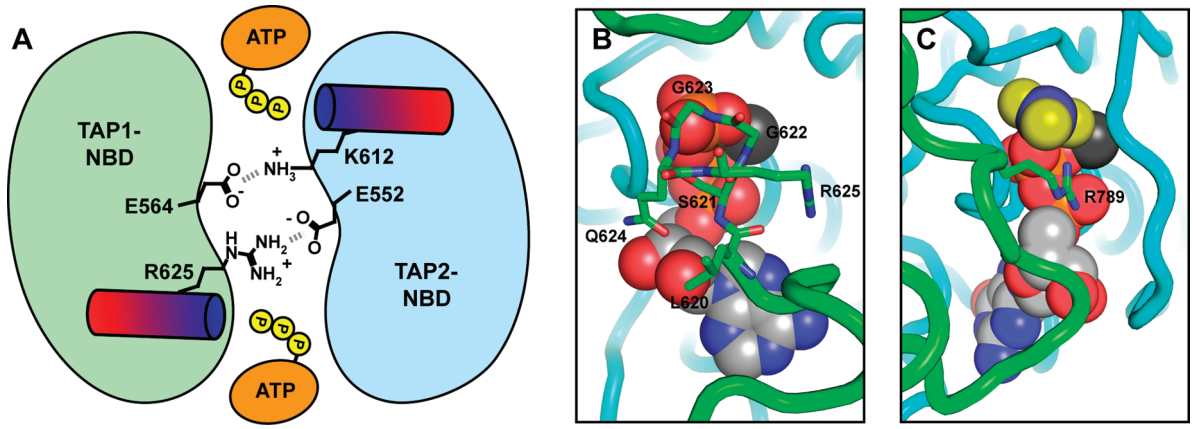

FIGURE 7: Important interactions at the TAP1-NBD/TAP2-NBD interface. (A) The closed NBD dimer is held together by contacts to the γ-phosphates from the signature motifs. The signature motif forms the first turn of an α-helix (cylinders) and sits flush against the γ-phosphate such that the partial positive charge of the helix macrodipole is orientated toward the ATP (blue indicates partial positive charge and red partial negative charge). A basic residue adjacent to the signature motif forms an interaction with an acidic residue from the Q-loop on the opposing NBD. (B) An active site of the ATP-bound TAP1-NBD homodimer (PDB entry 2IXE) (*14*). The signature motif (sticks) contacts and stabilizes ATP•Mg^{2+} (spheres) for hydrolysis. (C) Active site of RasGAP (green) bound to Ras (blue) (PDB entry 1WQ1) (*28*). GDP•AlF_3•Mg^{2+} is shown in space-filling spheres. The arginine finger (Arg789, shown in stick representation) of RasGAP contacts and stabilizes the nucleotide for hydrolysis.

are partially tolerated in the degenerate site but severely impair TAP activity when introduced into the consensus site (*15, 22, 23*). This could be explained if the interactions couple the two ATPase sites, such that if either interaction is lost, errors may occur during coordination of events. Both the TAP1-NBD and HlyB-NBD dimer stuctures exhibited one interaction constricting an adjacent cavity, while the second interaction was broken and the cavity enlarged (*14, 16*). This structural asymmetry demonstrates that the interactions are structurally coupled rather than independent. The opening and closing of the interactions could be tied to conformational changes anticipated during ATP hydrolysis, as the basic residues are in the proximity of ATP.

Unlike in the HlyB study (*16*), mutagenesis of the interacting residue pairs in the TAP1-NBD dimer does not disrupt ATP-dependent positive cooperativity in ATPase assays. Since NBD dimerization requires interaction of two ATP-bound subunits, any dimerization-dependent activity, including ATP hydrolysis, is expected to display at least some positive cooperativity with respect to both ATP and protein concentration. The higher positive cooperativity observed for HlyB-NBD versus TAP1-NBD (Hill coefficients h of 1.8 and 1.4, respectively) may indicate that HlyB-NBD has an additional cooperativity effect absent in TAP. Overall, it is unclear whether the discrepancies between the two studies reflect real differences between the respective transporters or are a product of different experimental designs. To address this, more studies will need to link data from isolated NBDs to the activity of the full transporter, as we have in part attempted to do here.

Of note, some experiments presented here utilized the TAP1-NBD homodimer, which has the advantage of being symmetric with a single type of ATPase site, ideal for studying different ATPase active site properties (*14*). Mutations to the TAP1-NBD Walker B or signature motifs reduce the protein's ATPase activity (*14*), indicating that the activity observed, while low, follows a catalytic mechanism similar to that of other ABC transporters. However, our ATPase and dimerization data must be considered with the caveat that they were not obtained from the physiological TAP1-NBD/TAP2-NBD heterodimer. This is mainly because isolated TAP2-NBD has weak affinity for ATP (*26*), making the in vitro formation of a physiological ATP-bound heterodimer from isolated NBDs technically challenging. However, the TAP1- and TAP2-NBDs are highly homologous (the rat TAP NBDs are 54% identical and 80% similar; Supporting Information, Figure S1), with most differences located within the helical subdomain and C-terminal tail, which is responsible for TAP2's low affinity for ATP (*26*). Further, a homology model of the TAP1-NBD/TAP2-NBD heterodimer places the charged residues investigated here within proximity of one another, as expected if they are to form electrostatic interactions (Figure S1B). Finally, previous studies using the TAP1-NBD dimer have successfully explained the behavior of full-length TAP mutants (*14*), and in this study, TAP1 and TAP2 residues predicted to interact from a TAP1-NBD crystal structure were shown to be functionally coupled in full-length TAP. However, it is possible that further investigations of a physiological heterodimer might reveal that these electrostatic interactions have a much stronger influence on ATPase activity or dimerization than proposed here.

All single mutations that disrupted the putative electrostatic interactions reduced TAP activity, but activity was partially rescued when a second mutation was introduced to restore the interaction in a switched orientation. This clearly demonstrates that the proposed interacting residues are functionally coupled. However, the rescue was only partial, and mutations to the basic residues (R625E of TAP1 and K612E of TAP2) were more deleterious than mutations to the acidic residues (E564K and E552R of TAP1 and TAP2, respectively). Hence, there is a preference for a specific orientation of the interactions. An important role for a basic residue at the position equivalent to position 625 of TAP1 is underscored by sequence conservation. A basic residue in this position is found in 66% of ABC transporters, while an acidic residue at the position equivalent to position 564 of TAP1 is less conserved (41%) (*16*). The basic residues Arg625 in TAP1 and Lys612 in TAP2 immediately follow the signature motif, which forms the first turn of an α-helix and sits flush against the γ-phosphate of ATP, such that the

positive helix macrodipole is directed toward and stabilizes the γ-phosphate (*4*) (Figure 7A). Arg625 and Lys612 likely contribute to the positive field directed toward ATP. In the TAP1-NBD dimer, Arg625 begins the second turn of the helix and is directed toward the ATP-associated Mg^{2+} ion and α- and β-phosphates (Figure 7B), perhaps explaining why asymmetry of the interactions in the HlyB-NBD dimer was observed only when magnesium was present (*16*).

Many oligomeric nucleotide hydrolases have composite active sites, in which two subunits both contribute residues for ATP hydrolysis. Frequently, one subunit binds the nucleotide triphosphate, while a second subunit inserts a basic arginine residue, termed an arginine finger, into the active site to promote hydrolysis (*27*). These proteins include members of the AAA+ ATPase family and the GTPase activating proteins that interact with Ras-related small GTPases (*27, 28*). In ABC transporters, the signature motif is analogous to this arginine finger. One ABC-type NBD contributes Walker A, Walker B, and switch motifs for ATP binding and hydrolysis, while the second NBD completes the active site by contributing the signature motif, positioned like the arginine finger of other hydrolases (Figure 7B,C). Furthermore, this interaction with the γ-phosphate by the second NBD is essential for hydrolysis and clearly parallels the requirement for an arginine finger in other ATPases and GTPases.

Abnormalities of TAP, including a reduced level of expression and a decreased level of substrate transport, have been documented in a number of cancers (*29, 30*). Loss of TAP activity is associated with a reduced level of surface class I MHC and allows cancerous cells to evade immune surveillance. A human TAP1 variant in which Arg648 (Arg625 in rat) is replaced with glutamine was found much more frequently in colon cancers with a decreased level of surface class I MHC compared to those with normal surface MHC levels (*29*). This variant had poor peptide transport activity (*29*), as we also observed in the analogous R625E rat transporter mutant (Figure 5). Our data here reveal that this arginine is part of an important intersubunit interaction, as well as possibly having other roles, such as contributing to the positive electrostatic field directed toward ATP in the active site.

By demonstrating the presence of interactions between the TAP NBDs, we provide further evidence that the NBDs of ABC transporters dimerize as observed in crystal structures, even for more complex heterodimeric transporters. A similar biochemical approach demonstrated that the NBDs of CFTR, the ABC transporter mutated in cystic fibrosis, also close to regulate channel opening (*31*). Patch clamp analyses further determined that the open CTFR channel state occurs when the predicted residues are interacting across the interface, indicating that a closed NBD dimer corresponds to the open channel state (*31*). Our data also raise interesting questions about other mammalian ABC transporters. Interfacial interacting residues homologous to those of TAP are conserved among all 11 human B-subfamily ABC transporters, which include TAP, MDR1, and BSEP. However, the C-subfamily transporters show a different and interesting arrangement. While two (MRP6 and MRP7) have both pairs of interfacial residues, eight of the 12 human C-subfamily members (MRP1−5, SUR1 and SUR2, and MRP8) have only one pair and it is always the pair near the consensus ATPase site. Several human A-subfamily members (ABCA6, ABCA10, and ABCA12) show the same striking arrangement. In some cases, the acidic residue in the degenerate site is replaced with glutamine, which may still form a hydrogen bonding interaction. When there is an electrostatic interaction associated with only one ATPase site, the asymmetry between the consensus and degenerate sites is reinforced. Our data demonstrate that these interactions are important for transport but have little influence on ATPase activity, at least for the isolated TAP1-NBD dimer, leading us to hypothesize that they may be involved in transmission of conformational signals. It then raises interesting questions about the transport mechanisms of C-subfamily members, in particular whether the distinct ATPase and dimerization properties of the consensus and degenerate ATPase sites are supplemented by distinct "transmission" properties during ATP hydrolysis. Further experiments will be required to investigate these ideas.

ACKNOWLEDGMENT

We thank Sze-Ling Ng for assistance with protein purification and members of the Gaudet lab, particularly Samer Haidar and Christopher Phelps, for discussions.

SUPPORTING INFORMATION AVAILABLE

Similarity between TAP1- and TAP2-NBDs shown on a sequence alignment and on a homology model of the ATP-bound TAP1-NBD/TAP2-NBD heterodimer (Figure S1). This material is available free of charge via the Internet at http://pubs.acs.org.

REFERENCES

1. Cheng, S. H., Rich, D. P., Marshall, J., Gregory, R. J., Welsh, M. J., and Smith, A. E. (1991) Phosphorylation of the R domain by cAMP-dependent protein kinase regulates the CFTR chloride channel. *Cell 66*, 1027–1036.
2. Procko, E., Raghuraman, G., Wiley, D. C., Raghavan, M., and Gaudet, R. (2005) Identification of domain boundaries within the N-termini of TAP1 and TAP2 and their importance in tapasin binding and tapasin-mediated increase in peptide loading of MHC class I. *Immunol. Cell Biol. 83*, 475–482.
3. Linton, K. J. (2007) Structure and function of ABC transporters. *Physiology 22*, 122–130.
4. Hopfner, K. P., Karcher, A., Shin, D. S., Craig, L., Arthur, L. M., Carney, J. P., and Tainer, J. A. (2000) Structural biology of Rad50 ATPase: ATP-driven conformational control in DNA double-strand break repair and the ABC-ATPase superfamily. *Cell 101*, 789–800.
5. Smith, P. C., Karpowich, N., Millen, L., Moody, J. E., Rosen, J., Thomas, P. J., and Hunt, J. F. (2002) ATP binding to the motor domain from an ABC transporter drives formation of a nucleotide sandwich dimer. *Mol. Cell 10*, 139–149.
6. Pinkett, H. W., Lee, A. T., Lum, P., Locher, K. P., and Rees, D. C. (2007) An inward-facing conformation of a putative metal-chelate-type ABC transporter. *Science 315*, 373–377.
7. Hvorup, R. N., Goetz, B. A., Niederer, M., Hollenstein, K., Perozo, E., and Locher, K. P. (2007) Asymmetry in the Structure of the ABC Transporter Binding Protein Complex BtuCD-BtuF. *Science 317*, 1387–1390.
8. Locher, K. P., Lee, A. T., and Rees, D. C. (2002) The *E. coli* BtuCD structure: A framework for ABC transporter architecture and mechanism. *Science 296*, 1091–1098.
9. Michalek, M. T., Grant, E. P., Gramm, C., Goldberg, A. L., and Rock, K. L. (1993) A role for the ubiquitin-dependent proteolytic pathway in MHC class I-restricted antigen presentation. *Nature 363*, 552–554.
10. Spies, T., and DeMars, R. (1991) Restored expression of major histocompatibility class I molecules by gene transfer of a putative peptide transporter. *Nature 351*, 323–324.

11. Groothuis, T. A., Griekspoor, A. C., Neijssen, J. J., Herberts, C. A., and Neefjes, J. J. (2005) MHC class I alleles and their exploration of the antigen-processing machinery. *Immunol. Rev. 207*, 60–76.
12. Kelly, A., Powis, S. H., Kerr, L. A., Mockridge, I., Elliott, T., Bastin, J., Uchanska-Ziegler, B., Ziegler, A., Trowsdale, J., and Townsend, A. (1992) Assembly and function of the two ABC transporter proteins encoded in the human major histocompatibility complex. *Nature 355*, 641–644.
13. Koch, J., Guntrum, R., Heintke, S., Kyritsis, C., and Tampe, R. (2004) Functional dissection of the transmembrane domains of the transporter associated with antigen processing (TAP). *J. Biol. Chem. 279*, 10142–10147.
14. Procko, E., Ferrin-O'Connell, I., Ng, S. L., and Gaudet, R. (2006) Distinct structural and functional properties of the ATPase sites in an asymmetric ABC transporter. *Mol. Cell 24*, 51–62.
15. Perria, C. L., Rajamanickam, V., Lapinski, P. E., and Raghavan, M. (2006) Catalytic site modifications of TAP1 and TAP2 and their functional consequences. *J. Biol. Chem. 281*, 39839–39851.
16. Zaitseva, J., Oswald, C., Jumpertz, T., Jenewein, S., Wiedenmann, A., Holland, I. B., and Schmitt, L. (2006) A structural analysis of asymmetry required for catalytic activity of an ABC-ATPase domain dimer. *EMBO J. 25*, 3432–3443.
17. Dawson, R. J., and Locher, K. P. (2006) Structure of a bacterial multidrug ABC transporter. *Nature 443*, 180–185.
18. Dawson, R. J., and Locher, K. P. (2007) Structure of the multidrug ABC transporter Sav1866 from *Staphylococcus aureus* in complex with AMP-PNP. *FEBS Lett. 581*, 935–938.
19. Taylor, J. S., Vigneron, D. B., Murphy-Boesch, J., Nelson, S. J., Kessler, H. B., Coia, L., Curran, W., and Brown, T. R. (1991) Free magnesium levels in normal human brain and brain tumors: ^{31}P chemical-shift imaging measurements at 1.5 T. *Proc. Natl. Acad. Sci. U.S.A. 88*, 6810–6814.
20. Lauvau, G., Gubler, B., Cohen, H., Daniel, S., Caillat-Zucman, S., and van Endert, P. M. (1999) Tapasin enhances assembly of transporters associated with antigen processing-dependent and -independent peptides with HLA-A2 and HLA-B27 expressed in insect cells. *J. Biol. Chem. 274*, 31349–31358.
21. Peh, C. A., Burrows, S. R., Barnden, M., Khanna, R., Cresswell, P., Moss, D. J., and McCluskey, J. (1998) HLA-B27-restricted antigen presentation in the absence of tapasin reveals polymorphism in mechanisms of HLA class I peptide loading. *Immunity 8*, 531–542.
22. Karttunen, J. T., Lehner, P. J., Gupta, S. S., Hewitt, E. W., and Cresswell, P. (2001) Distinct functions and cooperative interaction of the subunits of the transporter associated with antigen processing (TAP). *Proc. Natl. Acad. Sci. U.S.A. 98*, 7431–7436.
23. Alberts, P., Daumke, O., Deverson, E. V., Howard, J. C., and Knittler, M. R. (2001) Distinct functional properties of the TAP subunits coordinate the nucleotide-dependent transport cycle. *Curr. Biol. 11*, 242–251.
24. Jones, P. M., and George, A. M. (2007) Nucleotide-dependent allostery within the ABC transporter ATP-binding cassette: A computational study of the MJ0796 dimer. *J. Biol. Chem. 282*, 22793–22803.
25. Chen, J., Lu, G., Lin, J., Davidson, A. L., and Quiocho, F. A. (2003) A tweezers-like motion of the ATP-binding cassette dimer in an ABC transport cycle. *Mol. Cell 12*, 651–661.
26. Bouabe, H., and Knittler, M. R. (2003) The distinct nucleotide binding states of the transporter associated with antigen processing (TAP) are regulated by the nonhomologous C-terminal tails of TAP1 and TAP2. *Eur. J. Biochem. 270*, 4531–4546.
27. Ye, J., Osborne, A. R., Groll, M., and Rapoport, T. A. (2004) RecA-like motor ATPases: Lessons from structures. *Biochim. Biophys. Acta 1659*, 1–18.
28. Scheffzek, K., Ahmadian, M. R., Kabsch, W., Wiesmuller, L., Lautwein, A., Schmitz, F., and Wittinghofer, A. (1997) The Ras-RasGAP complex: Structural basis for GTPase activation and its loss in oncogenic Ras mutants. *Science 277*, 333–338.
29. Yang, T., Lapinski, P. E., Zhao, H., Zhou, Q., Zhang, H., Raghavan, M., Liu, Y., and Zheng, P. (2005) A rare transporter associated with antigen processing polymorphism overpresented in HLAlow colon cancer reveals the functional significance of the signature domain in antigen processing. *Clin. Cancer Res. 11*, 3614–3623.
30. Zheng, P., Guo, Y., Niu, Q., Levy, D. E., Dyck, J. A., Lu, S., Sheiman, L. A., and Liu, Y. (1998) Proto-oncogene PML controls genes devoted to MHC class I antigen presentation. *Nature 396*, 373–376.
31. Vergani, P., Lockless, S. W., Nairn, A. C., and Gadsby, D. C. (2005) CFTR channel opening by ATP-driven tight dimerization of its nucleotide-binding domains. *Nature 433*, 876–880.

BI7024854